

Patient-Specific Pre-Treatment VMAT Plan Verification Using Gamma Passing Rates

M. Z. Arsalan^{1,2*}, M. B. Kakakhe², M. Shamshad³, T. A. Afridi^{2,4}

¹Medical Physics Division, Atomic Energy Medical Center, Karachi (AEMC-K), Sindh, Pakistan

²Department of Physics and Applied Mathematics, Pakistan Institute of Engineering and Applied Sciences (PIEAS), Islamabad, Pakistan.

³Danish Centre for Particle Therapy (DCPT), Denmark

⁴Medical Physics Division, Atomic Energy Cancer Hospital NORIN, Nawabshah, Sindh, Pakistan

ARTICLE INFO

Article history:

Received 29 July 2022

Received in revised form 4 December 2022

Accepted 13 December 2022

Keywords:

VMAT

Treatment planning system

Gamma analysis

Octavius 4D setup

Gamma acceptance criteria

ABSTRACT

Continuous gantry motion, continuous beam modulation, and variable dose rate are used in volumetric modulated arc therapy (VMAT) to obtain highly conformal radiation therapy dose distributions. Several errors during daily radiation therapy treatment can be sources of uncertainties in dose delivery. These errors include monitor unit calculation errors and other human mistakes. Due to the uncertainties in the excessively modulated VMAT plan, the intended dose distribution is not delivered perfectly, leading to a mismatch between the measured and planned dose distributions. This necessitates an extensive and effective quality assurance (QA) program for both machine and patient. In this study, VMAT QA plan verification of 62 head and neck (H&N) and 19 prostate cases was done using Octavius 4D setup with its associating VeriSoft gamma analysis software. The plans showed a maximum 3D gamma passing rate with 4 mm/3 % gamma acceptance criteria, i.e., 99.7 % for the H&N cancer cases and 99.5 % for the prostate cancer cases. Local gamma analysis was also performed for both regions. Furthermore, 2D and volumetric gamma analyses were also carried out. Gamma analysis with respect to different axis was also carried out. It was known that the transversal axis showed the highest gamma passing rate in both H&N and prostate cases, i.e., 99.17 % and 98.3 %, respectively. The transverse axis came to be a better fit for the planned dose distribution.

© 2023 Atom Indonesia. All rights reserved

INTRODUCTION

Cancer is a leading global disease. Cancer type, location, and progression status are the main factors that are considered in selecting an appropriate treatment. One such treatment is radiotherapy, in which high-energy ionizing radiations are used to treat the cancer. Nowadays fractionated schemes like external beam radiotherapy (EBRT) or brachytherapy (BT) which makes advantageous use of the radiobiological difference between a cancer cell and normal cells are employed. One of the arc-based EBRT techniques is referred to as volumetric modulated arc therapy (VMAT). This has twofold motivations. First, all gantry angles are used for patient irradiation instead of a few discrete angles. Second, VMAT has shorter treatment times as the treatment beam is ON during

rotation [1]. VMAT is an extension of traditional intensity modulated radiation therapy (IMRT). Continuous gantry motion, continuous beam modulation, and variable dose rate are used in VMAT to obtain highly conformal dose distribution [1]. The lack of technological advances has been a major hindrance to the clinical implementation of VMAT. Rotational delivery with variable dose rate options was introduced by both Elekta and Varian in their linear accelerators in the late 2000s [2]. Optimal dose distributions in VMAT are due to modulation of the photon beam, but excessively modulating a VMAT plan can create discrepancies between planned and delivered dose distributions [3]. Such excessively modulated VMAT plans have more mechanical and dose calculation uncertainties [3,4]. The accuracy of dose calculation using irregularly-shaped photon beams or small field beams with current dose calculation algorithms is limited; therefore, the intended dose distribution

*Corresponding author.

E-mail address: ziamedicalphysicist@gmail.com

DOI: <https://doi.org/10.55981/aij.2023.1261>

may not be delivered accurately [4]. Mechanical uncertainties increase with an increase of VMAT plan modulation due to increase of complications in the beam delivery system and mechanical movements, i.e., gantry rotation and MLC positioning [5].

Several errors during daily treatment contribute to dose delivery uncertainties, such as monitor unit calculation in the treatment planning system (TPS) and other human errors. The human error will possibly only affect one treatment session, but the TPS calculation will affect the whole treatment course and most likely many patients. TPS-related errors are systematic errors that include algorithm limitations, model settings, and alignment and modeling of QA phantoms in the TPS. Most human errors, i.e., patient adjustment, positioning and fixation devices, and patient movement are easily corrected after detection, and uncorrectable ones provide information about system limitations. Machine malfunctions also become a major source of error in dose delivery and the cause of extra dose to the patient if it remains undetected. VMAT plans are highly optimized so even a slight deviation of gantry angle/position, MLC shape/position, and couch parameters from the optimized parameters lead to unexpected clinical outcomes. Wang et al. [6] investigated the consequences of MLC positional errors in VMAT and concluded that a cautious MLC calibration procedure is highly recommended for accurate dose delivery. Their results showed that positional error of MLC beyond ± 0.3 mm influenced modulated dose distributions significantly. Milan et al. [7] evaluated the impact of MLC and gantry sag in VMAT their results showed a decrease in dose uniformity to PTV and overall degradation of plan quality. Raghavendra et al. [8] have discussed the effects of collimator and gantry positional errors on VMAT and concluded that a one-degree error in collimator angle affects OAR doses more significantly compared to a one-degree error in gantry angle.

Due to uncertainties in the excessively modulated VMAT plan, the intended dose distribution is not perfectly delivered, which causes a discrepancy between the actual measured and planned dose distribution. This necessitates an extensive and effective quality assurance (QA) program for both the machine and the patient. In clinical settings, patient-specific and pretreatment quality assurance for each VMAT plan is highly recommended [9,10]. Patient quality assurance procedures are usually end-to-end tests that are commonly expected to trace errors, which are clinically relevant and can occur at any point in the treatment chain. The QA protocol related to the

patient is a crucial step that requires a careful pretreatment check. For treatment techniques such as VMAT or helical tomo-therapy, a reliable method for routine pretreatment verification is highly desirable. For pretreatment verification, a phantom approach is generally used; dose is recalculated in a phantom setup after transferring the treatment plan to the phantom. The phantom approach involves the verification plan's preparation using the same beam parameters as that of the patient plan and delivering it to the phantom. TPS-calculated and phantom measured doses are then compared with the help of the gamma index [11].

Treatment plans are usually evaluated using dosimetric metrics, i.e., by comparing dose-volume histograms (DVH), dose profiles, isodose curves, monitor units (MU), homogeneity index (HI), gradient index (GI), and conformity index (CI). Some treatment plans are also evaluated radiologically by comparing equivalent uniform doses (EUD). For quantization of the complexity of a treatment plan, metrics such as modulation complexity scores, the edge metric and leaf motion (average) per degree of gantry rotation are used [12]. The gamma index is the most common tool used to evaluate treatment plan deliverability [13]. A comprehensive study on treatment plan verification metrics has been done by Diamantopoulos et al. [14]. It represents a general description of each dose comparison technique along with its advantages and rationale for its development. Various researchers have used different methods and QA tools to collect dose data of different VMAT plans and then evaluated them with the help of the gamma index. A comparison study between different IMRT/VMAT QA systems was conducted by Hussein et al. [10] using the gamma index. The reliability of the gamma index was investigated along with the impact of low-resolution detector arrays. It was concluded that it is very essential to understand the responses and limitations of the gamma index combined with the tools/equipment used.

Several researchers have used the PTW 2D detector arrays such as seven29, 1000 (SRS), and 1500 in the PTW OCTAVIUS 4D setup and its accompanying VeriSoft software for gamma analysis. This setup and associated software are used to compare the planned and delivered dose distributions [15]. The main features of the Octavius 4D system, as concluded by many authors, are its directional independence with respect to the gantry angle and 3D dose reconstruction in its rotational unit [16-20].

The gamma analysis evaluates dose distributions quantitatively by calculating the gamma index value of each point in the dose distribution.

Then, it uses two acceptance criteria to evaluate the difference between the dose distributions. The first criterion is distance-to-agreement (DTA) in mm, and the second is the dose difference in %. This study aims to find acceptance criteria for head and neck (H&N) and prostate VMAT plans in our clinical setting using the Octavius 4D system. Due to the elevated incidence of H&N and prostate cancers, these areas were selected for the study.

METHODOLOGY

Patient selection

A total of 81 patients, consisting of 62 H&N cancer patients and 19 prostate cancer patients at the Institute of Nuclear Medicine and Oncology (INMOL), Lahore, Pakistan, were selected for this study. Patients with gross tumor sizes between 3-7 cm³ were selected. Each patient underwent CT simulation using the Toshiba Aquilion 16 CT scanner. Multiple transverse CT slices of 5 mm thickness were obtained for each patient.

Treatment and verification planning

All cases were planned with the objective in mind so as not to miss the target from any angle. Each VMAT plan was optimized using the photon optimizer algorithm (version 15.6.04) and the subsequent dose calculation was carried out using the Anisotropic Analytical Algorithm (AAA) (version 15.6.04). After optimizing the VMAT plan for each patient, a verification plan on Octavius phantom CT was also generated as shown in Fig. 1.

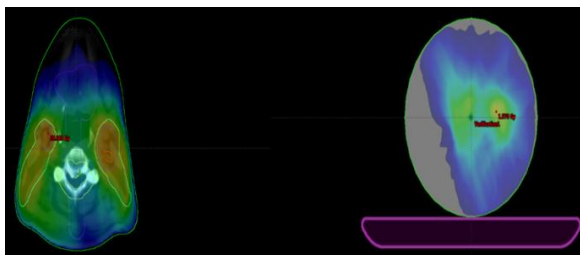


Fig. 1. H&N VMAT on patient anatomy (left), and verification plan on Octavius 4D phantom CT (right).

The Octavius 4D phantom CT is provided by the vendor (PTW Freiburg, Germany), including the setup. However, CT slices of the phantom generated in the clinic can also be used. The only difference between the verification plan and the actual plan is the patient anatomy which is absent in the verification plan. The rest of the parameters, such as the number arcs and the monitor units are the same.

Octavius 4D setup

The Octavius 4D setup is a motorized rotation platform used for VMAT and IMRT QA and plans verification developed by PTW of Freiburg, Germany. Octavius 4D setup consists of: (1) a cylindrical phantom; (2) a 2D detector array; (3) an inclinometer; and (4) a control and detector interface. The cylindrical phantom is also called the Octavius phantom or Octavius rotational unit. It is composed of polystyrene having a physical density of 1.05 g/cm³ and a relative electron density of 1.016 g/cm³. It has a reported accuracy of $\pm 1^\circ$ and can reach a maximum rotation speed of 18°/s.

For dose data collection, a 2D detector array is used with the Octavius phantom. The Octavius phantom and its 2D detector arrays have been widely investigated by many researchers [16-20]. The choice of the 2D detector array depends on the user's preferences and clinical requirements. In this study, an Octavius 729 2D detector array was used. The detector array was inserted into the middle cavity of the phantom such that the middle of the detector array, i.e., the central chamber, is in the center of the phantom as shown in Fig. 2. The inclinometer is a wireless device that is attached to the gantry, and it sends gantry angle information to the Octavius phantom control unit via Bluetooth signals.



Fig. 2. The Octavius 4D rotational unit and Octavius 729 2D detector array.

Dose calculation

The charge data (later converted to dose data by software using appropriate factors) collected using a 2D detector array (Octavius 4D system) was used to generate a 3D dose distribution using VeriSoft software. Measured depth dose curves (PDDs) and Octavius phantom CT scans are used by Verisoft for 3D dose reconstruction. Contrary to ArcCHECK and Delta-4, VeriSoft software reconstructs a 3D dose grid (26 cm × 26 cm for the 729 detector array) without using TPS dose information [16]. This 3D dosimetric data grid

allows qualitative comparison of both plans along with the quantitative gamma analysis evaluation. The VeriSoft software allows 2D, 3D, and volumetric gamma analysis. and therefore, the QA results of this test tool are completely independent of the treatment plan.

Verification setup and plan verification

Figure 3 depicts the standard verification setup that was used in the verification of all the VMAT plans reported in this study. The Octavius 4D phantom was always placed on the couch with the table tolerance limits in mind (i.e., maximum 8 cm couch shift from the normal position (0,0,0)).



Fig. 3. Standard verification setup, Octavius 4D phantom in facing away from the gantry.

As it was reported that detector warm-up and cool-down affect the detector stability and resultantly the dose data [17,18,21], so a warm-up dose of 500 MU and 200 MU using 20 cm × 20 cm field size was delivered to the Octavius 4D phantom in the standard setup to minimize the uncertainty in the dose data collection.

Gamma analysis

The VeriSoft software performs 3D gamma analysis by comparing volumes, and 2D gamma analysis by comparing planes of the phantom measured and TPS calculated plans, respectively. Furthermore, it performs gamma analysis in all three major axes (sagittal, axial, and coronal) and the whole volume (volumetric) both locally and globally. Usually, local and global gamma passing rates are calculated as both have their pros and cons. The gamma analysis was performed using VeriSoft software package. Gamma index was calculated for reconstructed dose distribution in all three axes, 2D, and 3D. The gamma analysis was also performed using different acceptance criteria, i.e., 3 mm/3 %, 2 mm/2 %, 1 mm/1 %, and 2 mm/3 %. Both the local and the global gamma analysis was performed using these criteria.

RESULTS AND DISCUSSION

Table 1 presents percentages of 3D and 2D global gamma passing rates calculated using different acceptance criteria for H&N and prostate cases. The highest 3D gamma passing rate was 99.7 % and 99.5 % in H&N and prostate cases respectively with 4 mm/3 % acceptance criteria. The 2D gamma passing rate was also highest with the 4 mm/3 % acceptance criteria, i.e., 98.7 % for H&N and 97.8 % for prostate cases.

Table 1. Gamma analysis (global) of H&N and prostate cases (mean ± standard deviation).

| | H&N | | Prostate | | |
|--------------|---------|------------|------------|------------|------------|
| | 3D | 2D | 3D | 2D | |
| N=62 N=19 | 4mm/3 % | 99.7±0.34 | 98.7±1.56 | 99.5±0.66 | 97.8±2.11 |
| | 3mm/3 % | 99.17±0.93 | 97.59±.38 | 98.3±1.86 | 95.95±3.24 |
| | 2mm/2 % | 93.35±4.81 | 88.55±7.86 | 91.38±6.49 | 84.7±7.88 |
| | 1mm/1 % | 65.2±4.36 | 58.4±14.9 | 62.5±16.4 | 54.95±19.4 |

The lowest gamma passing rate was observed with an acceptance criterion of 1 mm/1 % in the 2D gamma analysis, i.e., 58.4 % for H&N and 54.9 % for prostate cases. The 3D gamma passing rate with the same acceptance criterion was also lower, i.e., 65.2 % for H&N and 62.5 % for prostate cases. Table 2 shows the 2D and the 3D local gamma passing rates in percentages for the H&N and prostate cases against different acceptance criteria.

Table 2. Gamma analysis(local) of H&N & Prostate cases (mean ± standard deviation).

| | H&N | | Prostate | | |
|--------------|---------|-----------|------------|-----------|------------|
| | 3D | 2D | 3D | 2D | |
| N=62 N=19 | 4mm/3 % | 97.3±2.32 | 86.5±11.47 | 96.7±3.80 | 79.4±18.4 |
| | 3mm/3 % | 92.9±4.84 | 79.7±12.62 | 91.7±7.04 | 70.1±18.2 |
| | 2mm/2 % | 78.4±10.2 | 61.17±12.7 | 77.9±13.2 | 51.7±16.03 |

The highest 3D local gamma passing rates were 97.3 % and 96.7 in H&N and prostate cases, respectively, with 4 mm/3 % acceptance criteria. The 2D local gamma passing rate was also highest with the 4 mm/3 % acceptance criteria, i.e., 86.5 % for H&N and 79.4 % for prostate cases.

The lowest gamma passing rate was observed with an acceptance criterion of 2 mm/2 % in the 2D gamma analysis, i.e., 61.1 % for H&N and 51.7 % for prostate cases. The 3D gamma passing rate with the same acceptance criterion was also lower, i.e., 78.4 % for H&N and 77.9 % for prostate cases.

Figure 4 shows the 3D and 2D gamma passing rates in different axes which were obtained by comparing different axes of TPS-calculated dose distribution and phantom-measured dose distribution. The global 3D and 2D gamma analysis with an acceptance criterion of 3 mm/3 % was used for this evaluation. The highest 3D and 2D gamma passing rates for both H&N and prostate cases were observed for the transverse axis mainly. In the H&N cases, the highest gamma passing rate was 99.17 % and 97.5 % for global and local gamma analysis, respectively, in the transverse axis. For the prostate cancer, the 3D gamma's highest passing percentage was 98.3 %. The 2D gamma analysis results in prostate cases showed the maximum passing percentage of 96.25 % in the sagittal axis.

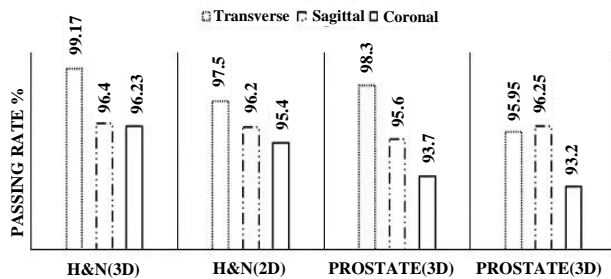


Fig. 4. Gamma passing rates in different axes (Transverse, Sagittal, Coronal).

All the calculated results showed that the gamma passing rate depends on several factors, i.e., the degree of fluence modulation in VMAT plans and the acceptance criterion used. The same result is reported by Jong Min Park et al. who describe that gamma analysis depends upon several factors, i.e., dosimeters, acceptance criteria, LINAC type, and VMAT plan modulation degree [22]. A greater fluence modulation between two detectors results in a lower recorded dose than the calculated which leads to dose disagreement [23].

The resolution of the detector array has a vital role in the gamma passing rate. The higher the number of detectors, the higher the resolution, and

the higher the gamma passing rates even with strict acceptance criteria [18]. The strict criteria, i.e., 1 mm/1 %, can be ruled out as it is arguable on the following reasons. First, statistical fluctuations and dosimetric errors are very dominant for these criteria. Second, the acceptable level of gamma passing rate should be different for this criterion concerning the other, lenient acceptance criteria, i.e., 2 mm/2 % and 3 mm/3 % [24]. Furthermore, our results for the acceptance criterion of 1 mm/1 % denotes the maximum standard deviation, indicating its statistical randomness.

Tables 1 and 2 show that the 2D gamma analysis results are always lower than the 3D gamma analysis results because in the 3D gamma analysis neighboring slices are also taken into account while performing slice-by-slice evaluation. The extra dimension increases the search radius leading to a lower gamma index and higher passing rates even if the same acceptance criteria are used for QA [25]. On the contrary, in the 2D gamma analysis, each slice is completely independent of its surrounding volume, which results in a higher gamma index and therefore in a lower passing rate. The 2D gamma analysis results thus strongly depend on the plane chosen for evaluation [25].

Figure 4 shows that the gamma passing rate for the transverse axes are always higher compared to the other axes. The results are in agreement with those reported by the vendor. The transverse CT slice of the patient are used for a treatment plan, so the transversal view relates to them easily. The two other axes are digitally reconstructed so they are prone to errors.

The local gamma passing rates tend to highlight failure in low-dose regions and in high-dose gradients [13]. Our evaluated VMAT plans have random passing rates when either local 2D or 3D gamma analysis is performed, and the passing rates are lower with tight acceptance criteria as seen in Tables 1 and 2. No specific pattern is observed but the lower local gamma index is expected as VMAT plans have higher dose gradients and lower dose regions. The global gamma index masks the failures that are highlighted by the local gamma index instead it highlights errors in higher-dose regions [13]. Our results for the global 2D or 3D gamma index show higher gamma passing rates which means our plans have fewer errors in high-dose regions. The 3D gamma index has a lower value than the 2D gamma index which is the result of the 3rd extra dimension and larger search radius. One of the main causes of lower 2D gamma results both locally and globally is due to setting up error that has the potential to cause impact on it. After all, in 2D gamma index analysis, no data from the plane

above or below the measuring plane is available to help DTA to compensate for these setup errors in that dimension [26].

The overall gamma passing rates were higher in H&N cases than that in the prostate cases. These results are in contrary to what was expected as in H&N treatment small targets require high beam modulation leading to lower gamma passing rates [25,27]. The few main reasons that could justify the lower gamma passing rates in prostate cases are the higher dose per fraction compared with H&N cases, and the larger number of MU compared to H&N cases leading to more MLC miscarriage or leakage, when in turn leads to significant extra dose [28,29]. Another reason is the more dose gradient in prostate cases compared to H&N cases [22]. The 729 2D-detector array is unable to resolve the dose gradients in prostate cases because of its lower resolution [30,31].

CONCLUSION

In this study, the PTW Octavius 4D setup was found to be a reliable QA tool for patient-specific VMAT plan analysis along with VeriSoft software that can be used for 2D, 3D, and volumetric gamma analysis. The global gamma analysis yielded better passing rates compared to the local gamma analysis due to larger low-dose regions in VMAT plans. An important finding was that the transverse axis showed to be a better fit for the planned dose distribution. The difference between 3D and 2D gamma results was elevated with the increase in DTA and dose difference criterion. All chosen VMAT plans showed more than 95 % gamma passing rate with a 3 mm/3 % acceptance criterion. H&N and prostate cases showed a gamma passing rate of 97 % and 98 % in the transversal axis, respectively.

The use of stringent criteria is strongly suggested to point out the maximum errors/mismatch between the planned and delivered dose distributions. As the gamma analysis helps only in checking plan deliverability, a separate dosimetric check is always required so that the treated region receives the prescribed dose accurately. Furthermore, the acceptance criteria used to evaluate VMAT plans should be chosen according to the treated anatomical region and the resolution of the chosen detector. A higher resolution detector array is highly recommended for better gamma analysis with stringent acceptance criteria. A high-resolution detector array will be able to resolve steep dose gradients and will result in less mismatch between the planned and delivered dose distributions and will correctly point out delivery errors.

ACKNOWLEDGMENT

The authors are wholeheartedly thankful to staff members of the Medical Physics Division of AECH-INMOL, Lahore, and DPAM-PIEAS, Islamabad, for their support and assistance throughout this research.

AUTHOR CONTRIBUTION

Mr. Muhammad Zia-ul-Islam Arsalan is the main author of this research article. He is presently serving as Senior Medical Physicist at Atomic Energy Medical Centre (AEMC) Karachi. He completed his MS in Medical Physics from PIEAS, Islamabad. He has very keen interest in the field of Radiation Dosimetry, Treatment Planning, Radiation Protection, Nuclear Medicine, and Radioactive Waste Management.

REFERENCES

1. E. Kamperis, C. Kodona, K. Hatzioannou *et al.*, *Int. J. Radiat. Oncol. Biol. Phys.* **106** (2020) 182.
2. F. M. Khan, P. W. Sperduto and J. P. Gibbons, *Khan's Treatment Planning in Radiation Oncology: Lippincott Williams & Wilkins*, (2021).
3. M. Antoine, F. Ralite, C. Soustiel *et al.*, *Phys. Medica* **64** (2019) 98.
4. D. P. Goodwin, *Point dose measurements in VMAT: an investigation of detector choice and plan complexity*. M. Sc. Thesis, University of Canterbury (2017).
5. R. Wang, Y. Du, K. Yao *et al.*, *Phys. Medica* **71** (2020) 14.
6. Y. Wang, X. Pang, L. Feng *et al.*, *Phys. Medica* **47** (2018) 112.
7. T. Milan, G. Grogan, M.A. Ebert *et al.*, *Med. Phys.* **46** (2019) 1984.
8. R. Holla, V.A. Ravikumar and B. Pillai, *Med. Phys.* **40** (2013) 368.
9. S. Michiels, K. Poels, W. Crijns *et al.*, *Radiother. Oncol.* **128** (2018) 479.
10. M. Hussein, P. Rowshanfarzad, M.A. Ebert *et al.*, *Radiother. Oncol.* **109** (2013) 370.
11. R. Mahmood, A. Babier, A. McNiven *et al.*, *Automated Treatment Planning in Radiation Therapy using Generative Adversarial Networks*, *Proceeding of the 3rd Machine Learning for Healthcare Conference*, PMLR 85 (2018) 484.

12. P. D. H. Wall and J. D. Fontenot, *Phys. Medica* **87** (2021) 136.
13. S. C. Peet, L. Yu, S. Maxwell *et al.*, *Phys. Medica* **78** (2020) 166.
14. S. Diamantopoulos, K. Platoni, G. Patatoukas *et al.*, *Phys. Medica* **67** (2019) 107.
15. V. Wyrwoll, B. Delfs, M. Lapp *et al.*, *Nucl. Instrum. Methods Phys. Res. Sect. A* **987** (2021) 164831.
16. B. Pal, A. Pal, S. Bag *et al.*, *Phys. Medica* **91** (2021) 18.
17. A. G. Ibrahim, I.E. Mohamed and H.M. Zidan, *Int. J. Med. Phys., Clin. Eng. Radiat. Oncol.* **7** (2018) 438.
18. D. Mönnich, J. Winter, M. Nachbar *et al.*, *Phys. Med. Biol.* **65** (2020) 1.
19. C. Q. Garcia, E. C. Solis, J. V. Salazar *et al.*, *Rev. Mex. Fis.* **67** (2021) 061101.
20. E. Decabooter, A. C. C. Swinnen, M. C. Öllers *et al.*, *Br. J. Radiol.* **94** (2021) 20210473.
21. B. Chand, M. Kumar and M. Kumar, *Eur. J. Mol. Clin. Med.* **7** (2020) 3595.
22. J. M. Park, J. Kim, S.-Y. Park *et al.*, *Radiat. Oncol.* **13** (2018) 1.
23. I. A. P. I. Gayatri, A. D. Handika, W. E. Wibowo *et al.*, *Appl. Radiat. Isot.* **188** (2022) 110415.
24. M. El Kafhali, M. Khalis, M. Tahmasbi *et al.*, *Phys. Med.* **12** (2021) 100044.
25. A. Chen, J. Zhu, N. Wang *et al.*, *Phys. Medica* **90** (2021) 134.
26. S. Zouiri, M. Tantaoui, M. El Hassani *et al.*, *Validation of Monaco Treatment Planning System for Intensity Modulated Radiation Therapy (IMRT) and Volumetric Modulated Arc Therapy (VMAT®) on ELEKTA Infinity™ Linear Accelerator*, *E3S Web Conferences* **297** (2021) 01014.
27. M. Chun, H. J. An, O. Kwon *et al.*, *Phys. Medica* **62** (2019) 83.
28. U. Yoshihiro, O. Shingo, I. Masaru *et al.*, *Br. J. Radiol.* **91** (2018) 1.
29. Y. C. Lee and Y. Kim, *Int. J. Med. Phys., Clin. Eng. Radiat. Oncol.* **10** (2021) 16.
30. A. Bruschi, M. Esposito, S. Pini *et al.*, *Phys. Medica* **49** (2018) 129.
31. W. Woon, P. B. Ravindran, P. Ekayanake *et al.*, *J. Appl. Clin. Med. Phys.* **19** (2018) 230.